

# Characterization of ALD Beryllium Oxide as a Potential High- $k$ Gate Dielectric for Low-Leakage AlGaIn/GaN MOSHEMTs

DEREK W. JOHNSON,<sup>1,6</sup> JUNG HWAN YUM,<sup>2</sup> TODD W. HUDNALL,<sup>3</sup>  
RYAN M. MUSHINSKI,<sup>3</sup> CHRISTOPHER W. BIELAWSKI,<sup>4</sup>  
JOHN C. ROBERTS,<sup>5</sup> WEI-E WANG,<sup>2</sup> SANJAY K. BANERJEE,<sup>4</sup>  
and H. RUSTY HARRIS<sup>1,7</sup>

1.—Texas A&M University, College Station, TX 77843, USA. 2.—SEMATECH, 2706 Montopolis Dr., Austin, TX 78741, USA. 3.—Texas State University, 601 University Drive, San Marcos, TX 78666, USA. 4.—University of Texas at Austin, 10100 Burnet RD, Austin, TX 78758, USA. 5.—Nitronex Corporation, 2305 Presidential Drive, Durham, NC 27703, USA. 6.—e-mail: dwjohnson87@gmail.com. 7.—e-mail: rusty.harris@tamu.edu

The chemical and electrical characteristics of atomic layer deposited (ALD) beryllium oxide (BeO) on GaN were studied via x-ray photoelectron spectroscopy, current–voltage, and capacitance–voltage measurements and compared with those of ALD Al<sub>2</sub>O<sub>3</sub> and HfO<sub>2</sub> on GaN. Radiofrequency (RF) and power electronics based on AlGaIn/GaN high-electron-mobility transistors are maturing rapidly, but leakage current reduction and interface defect ( $D_{it}$ ) minimization remain heavily researched. BeO has received recent attention as a high- $k$  gate dielectric due to its large band gap (10.6 eV) and thermal stability on InGaAs and Si, but little is known about its performance on GaN. Unintentionally doped GaN was cleaned in dilute aqueous HCl immediately prior to BeO deposition (using diethylberyllium and H<sub>2</sub>O precursors). Formation of an interfacial layer was observed in as-deposited samples, similar to the layer formed during ALD HfO<sub>2</sub> deposition on GaN. Postdeposition anneal (PDA) at 700°C and 900°C had little effect on the observed BeO binding state, confirming the strength of the bond, but led to increased Ga oxide formation, indicating the presence of unincorporated oxygen in the dielectric. Despite the interfacial layer, gate leakage current of  $1.1 \times 10^{-7}$  A/cm<sup>2</sup> was realized, confirming the potential of ALD BeO for use in low-leakage AlGaIn/GaN metal–oxide–semiconductor high-electron-mobility transistors.

**Key words:** BeO, high- $k$  dielectric, GaN, gate leakage, MOS

## INTRODUCTION

Recent advancements in GaN-based high-electron-mobility transistor (HEMT) technology have enabled the realization of high-voltage<sup>1</sup> and/or high-frequency devices.<sup>2,3</sup> Whether because of high blocking voltages or aggressively scaled device dimensions (necessary for mm-wave operation), high internal electric fields develop and cause leakage currents. Minimization of these currents through optimization of the gate stack and the

dielectric/GaN interface has been the focus of much recent research.<sup>4–8</sup> Atomic layer deposited (ALD) beryllium oxide (BeO) has also received much attention, especially for Si- and GaAs-based metal–oxide–semiconductor (MOS) devices, due to its large band gap (10.6 eV), thermal stability, and self-cleaning characteristics.<sup>9–12</sup> Additionally, the high thermal conductivity of BeO (300 W/m K) makes it appealing for power applications. In this paper, ALD BeO on GaN is characterized for the first time. The BeO/GaN interface and the thermal stability of that interface are observed by x-ray photoelectron spectroscopy (XPS). Then, the leakage behavior is discussed based on BeO/AlGaIn/GaN metal–oxide–semiconductor

(Received May 2, 2013; accepted August 19, 2013;  
published online September 25, 2013)

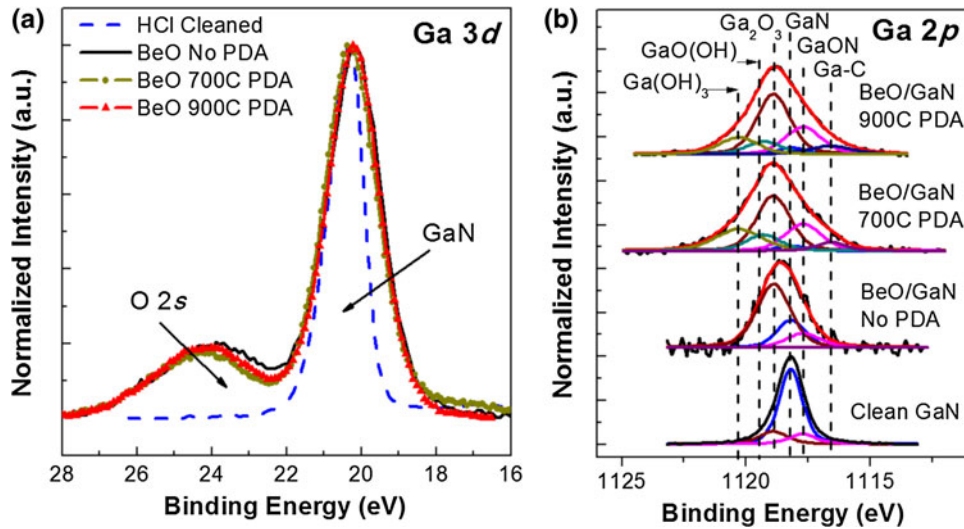


Fig. 1. HR XPS spectra of the Ga 3d (a) and Ga 2p<sub>3/2</sub> (b) binding energy levels. Ga 2p<sub>3/2</sub> spectra indicate formation of an interfacial layer which was exacerbated by the PDA process.

heterostructure (MOSH) capacitors and compared with the behavior of devices based on other gate dielectrics.

### EXPERIMENTAL PROCEDURES

Two different substrates were used for XPS sample preparation: GaN (5 μm) on sapphire, and GaN/AlGaIn/GaN (2 nm/17.5 nm/800 nm) on silicon. Substrates were cleaned in 1:1 deionized (DI) H<sub>2</sub>O:HCl for 2 min immediately prior to introduction into the ALD chamber. Three nanometers of BeO was deposited using H<sub>2</sub>O and Be(C<sub>2</sub>H<sub>5</sub>)<sub>2</sub> (DEBe) precursors at 250°C. DEBe is not commercially available and was synthesized using Grignard metathesis as previously described by Yum et al.<sup>11,12</sup> After blanket dielectric deposition, samples were annealed at various temperatures (0°C, 700°C, 900°C) in ambient N<sub>2</sub>. These temperatures emulate ohmic contact alloying anneals common in GaN HEMT processing. The samples were then analyzed using an Al K<sub>α</sub> x-ray source (1486.6 eV) and a hemisphere analyzer. The known N 1s binding energy of GaN (397.7 eV) was used for charge referencing of all spectra.<sup>13</sup>

MOSH capacitors were fabricated using the same 3-nm BeO film as the gate dielectric on AlGaIn/GaN on Si substrates so that the film properties would exactly match those observed via XPS. A ring structure was employed to negate the need for interdevice isolation. TaN gate contacts (100 nm) were deposited by evaporation, after which 100 nm of plasma enhanced chemical vapor deposition (PECVD) SiN was grown for surface state passivation. Contact windows were opened in the SiN/BeO using 7:1 buffered oxide etch (BOE). Ta/Al/Ta (10 nm/280 nm/17 nm) was evaporated and annealed at 575°C for ohmic contact formation.<sup>14</sup> Due to the excellent thermal stability of TaN, it is not expected to interact with the

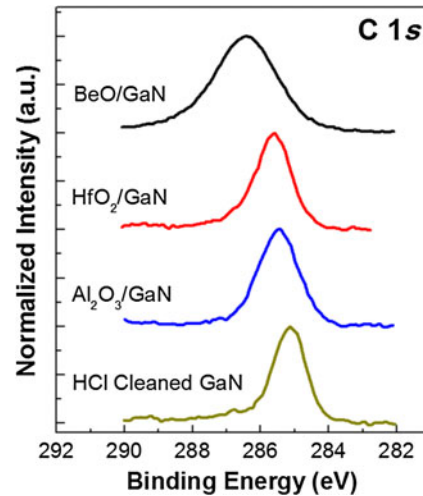


Fig. 2. HR XPS scans of the C 1s energy region of various ALD dielectrics deposited on GaN.

BeO at this temperature. Finally, capacitance (*C*-*V*) and conductance (*G*-*V*) versus bias voltage measurements were performed using an Agilent E4890A precision LCR meter, while a Hewlett Packard 4145 parameter analyzer was used for current-voltage (*I*-*V*) measurements. *C*-*V* and *G*-*V* characteristics were acquired while the gate voltage was swept from negative to positive and back (step = 0.05 V, dwell = 90 ms, 20 mV AC).

### RESULTS AND DISCUSSION

Figure 1 shows high resolution (HR) XPS spectra of the gallium 3d and 2p<sub>3/2</sub> cores. The Ga 2p<sub>3/2</sub> spectra are used for interpretation of the BeO/GaN interface due to the increased surface sensitivity of low-kinetic-energy electrons.<sup>15</sup> Minimal change was observed in the Ga 3d signal with respect to anneal

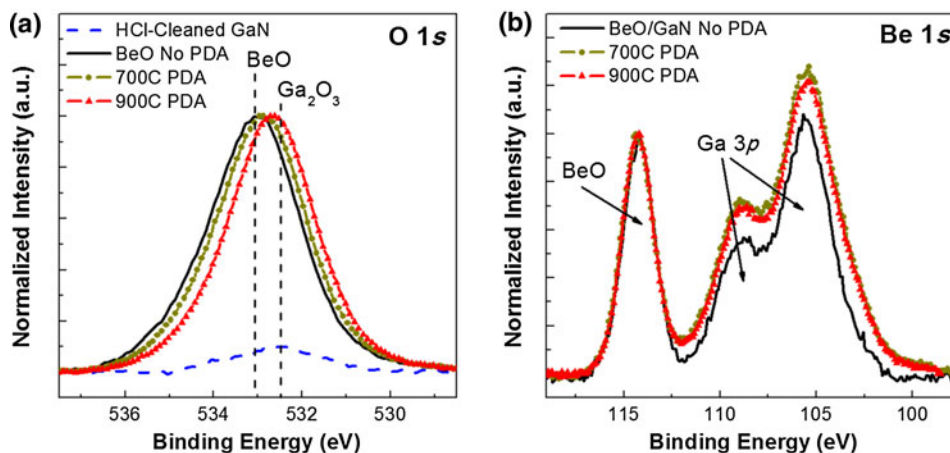


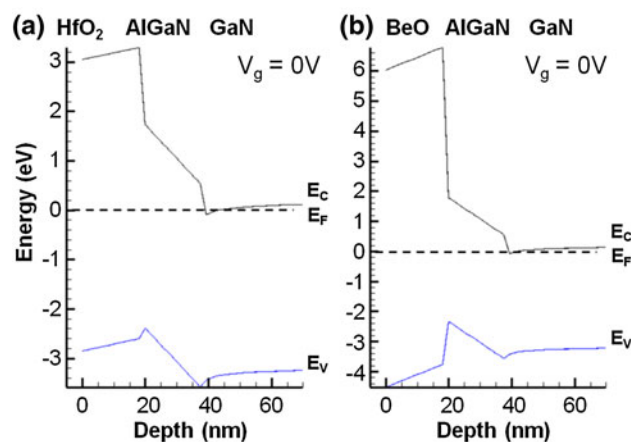
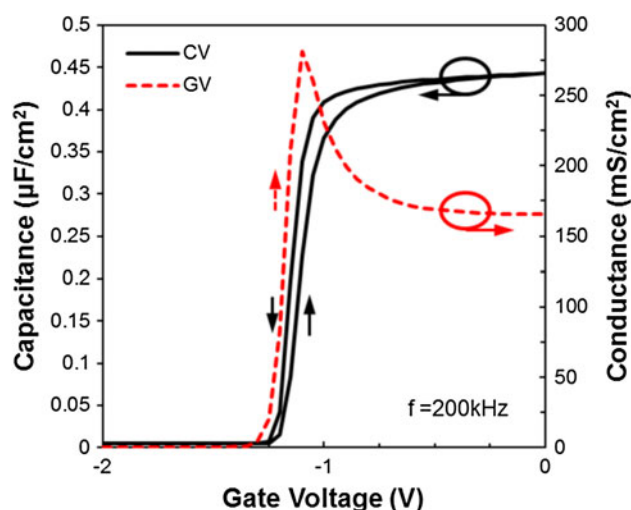
Fig. 3. HR XPS scans of O 1s (a) and Be 1s (b) energy regions.

temperature, but the Ga  $2p_{3/2}$  signal revealed that an interfacial layer formed during deposition and anneal, similar to that of ALD  $\text{HfO}_2$ .<sup>5</sup> Significant Ga oxide and  $\text{GaO}_x\text{N}_y$  ( $\text{Ga}^{1+}$ ) was deposited, and high-temperature annealing led to additional interfacial contamination by hydrogen and carbon, presumably originating from within the dielectric material. ALD BeO is known to have high carbon content due to the precursor synthesis process,<sup>11</sup> and this was also observed here (Fig. 2). As a result, ALD deposition of BeO using DEBe as a precursor is not found to be self-cleaning on GaN. The XPS spectra of BeO deposited on GaN/AlGaIn/GaN (not shown) exhibited a similar envelope. The interfacial layer is expected to contribute additional trap levels.

Figure 3 shows XPS scans of the Be 1s and O 1s energy regions. No change in the Be–O binding envelope was visible after the annealing process, confirming the strength of the BeO bond (asymmetry would be visible if decomposition occurred). However, the O 1s envelope shifted toward lower binding energy, indicating increased gallium oxide content. This implies that a significant concentration of unincorporated oxygen exists in the as-deposited dielectric. BeO is known to be an excellent diffusion barrier, so the oxygen is not believed to have originated outside of the film.<sup>9</sup> Angle-resolved XPS (ARXPS) indicated that Ga and N react with the unincorporated oxygen during the anneal, resulting in an intermixed  $\text{BeO-Ga}_2\text{O}_3\text{-O}_x\text{N}_y$  film (not shown).

Figure 4 presents a comparison of the band structures of  $\text{HfO}_2/\text{AlGaIn}$  and  $\text{BeO}/\text{AlGaIn}$  as calculated using numerical methods. The band alignment of  $\text{BeO}/\text{AlGaIn}$  was established using the valence-band offset (VBO) extracted from XPS spectra taken before and after dielectric deposition. The VBO was approximated as

$$\begin{aligned} \text{VBO} &= (E_{\text{Ga}3d}^{\text{AlGaIn}} - E_{\text{VBM}}^{\text{AlGaIn}}) - (E_{\text{Ga}3d}^{\text{BeO/AlGaIn}} - E_{\text{VBM}}^{\text{BeO/AlGaIn}}) \\ &= -1.9\text{eV}. \end{aligned}$$


 Fig. 4. Simulated band diagrams of  $\text{HfO}_2$  (a) and  $\text{BeO}$  (b) on an AlGaIn/GaN heterostructure. The predicted conduction-band offset of BeO on AlGaIn is approximately four times larger than that of  $\text{HfO}_2$ .

 Fig. 5. Normalized  $C$ - $V$  (solid) and  $G$ - $V$  characteristics (dashed) collected at 200 kHz.

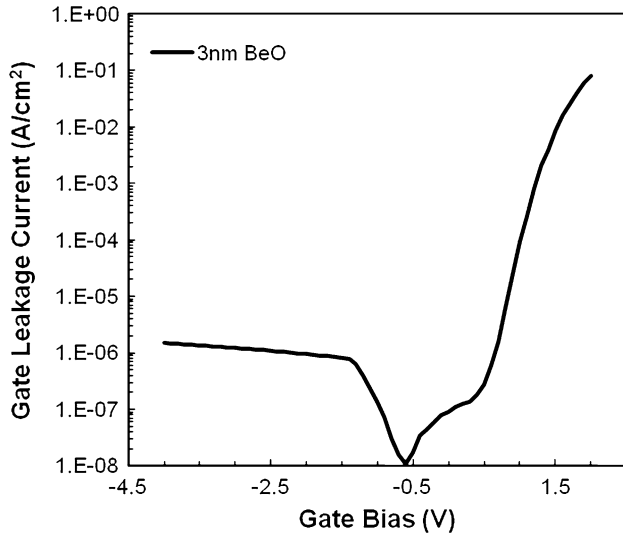


Fig. 6. Through-gate leakage current of BeO capacitor.

The predicted conduction-band offset (CBO) of  $\sim 4.5$  eV is nearly four times larger than that of  $\text{HfO}_2$  on AlGaIn. This highlights the potential performance gain of BeO. Capacitors were fabricated to determine the gate leakage performance and the impact of interfacial contamination.

The capacitance and conductance of a representative capacitor as a function of gate voltage are shown in Fig. 5. Counterclockwise hysteresis is observed, indicative of emptying of acceptor-type traps. The saturation capacitance ( $0.42 \mu\text{F}/\text{cm}^2$ ) leads to an effective dielectric constant of 8.5 for the gate dielectric. This is higher than the expected value of 6.8. We attribute this increase to formation of  $\text{Ga}_2\text{O}_3$  ( $\epsilon_r \approx 10$ ) within the dielectric layer as observed by ARXPS (not shown).<sup>16</sup> Charge trapping and frequency dispersion (not shown) were also observed during  $C$ - $V$  characterization, presumably due to interfacial contamination.

Figure 6 shows the normalized gate leakage current of a BeO capacitor. Leakage of  $1.1 \times 10^{-7} \text{ A}/\text{cm}^2$  was achieved in the forward-bias regime before the onset of tunneling. The early onset is due to the small thickness of the dielectric. This is better than the leakage of  $\sim 10^{-4} \text{ A}/\text{cm}^2$  realized using 5-nm ALD  $\text{HfO}_2$ <sup>17</sup> or 4.2-nm  $\text{SiO}_2$ <sup>18</sup> gate dielectrics, and is comparable to the leakage obtained using 15-nm ALD  $\text{Al}_2\text{O}_3$  ( $5 \times 10^{-7} \text{ A}/\text{cm}^2$ ).<sup>8</sup> Given the levels of contamination observed at the interface through XPS, we believe there is significant potential for further leakage reduction.

## CONCLUSIONS

ALD beryllium oxide has been investigated for use as a gate dielectric in AlGaIn/GaN MOSHEMTs.

Although the precursor synthesis process leads to significant carbon contamination of the dielectric film, low leakage performance was observed. BeO provides a viable gate dielectric alternative to  $\text{Al}_2\text{O}_3$  and deserves further exploration to optimize the BeO/GaN interface and to realize additional leakage current reduction.

## ACKNOWLEDGEMENTS

This work was supported in part by the National Excellence Fellowship, National Science Foundation Grant ECCS-1028910, and the Office of Naval Research Grant N00014-12-1-0971.

## REFERENCES

1. R. Chu, A. Corrion, M. Chen, R. Li, D. Wong, D. Zehnder, B. Hughes, and K. Boutros, *IEEE Electron Device Lett.* 32, 632–634 (2011).
2. J.W. Chung, K. Tae-Woo, and T. Palacios, *IEEE Int. Electron Devices Meeting (IEDM)* 30.2.1–30.2.4. (2010).
3. L. Dong Seup, G. Xiang, G. Shiping, D. Kopp, P. Fay, and T. Palacios, *IEEE Electron Device Lett.* 32, 1525–1527 (2011).
4. Y. Yuanzheng, H. Yue, Z. JinCheng, N. Jinyu, M. Wei, F. Qian, and L. Linjie, *IEEE Electron Device Lett.* 29, 838–840 (2008).
5. M.R. Coan, J.H. Woo, D. Johnson, I.R. Gatabi, and H.R. Harris, *J. Appl. Phys.* 112, 024508-024508-6 (2012).
6. R.D. Long, A. Hazeghi, M. Gunji, Y. Nishi, and P.C. McIntyre, *Appl. Phys. Lett.* 101, 5–241606 (2012).
7. N. Nepal, N.Y. Garces, D.J. Meyer, J.K. Hite, M.A. Mastro, and J.C.R. Eddy, *Appl. Phys. Express* 4, 055802 (2011).
8. M. Van Hove, S. Boulay, S.R. Bahl, S. Stoffels, K. Xuanwu, D. Wellekens, K. Geens, A. Delabie, and S. Decoutere, *IEEE Electron Device Lett.* 33, 667–669 (2012).
9. J.H. Yum, G. Bersuker, T. Akyol, D.A. Ferrer, M. Lei, P. Keun Woo, T.W. Hudnall, M.C. Downer, C.W. Bielawski, E.T. Yu, J. Price, J.C. Lee, and S.K. Banerjee, *IEEE Trans. Electron Devices* 58, 4384–4392 (2011).
10. J.H. Yum, T. Akyol, D.A. Ferrer, J.C. Lee, S.K. Banerjee, M. Lei, M. Downer, T.W. Hudnall, C.W. Bielawski, and G. Bersuker, *J. Vac. Sci. Technol. A: Vac. Surf. Films* 29, 061501–061506 (2011).
11. J.H. Yum, T. Akyol, M. Lei, D.A. Ferrer, T.W. Hudnall, M. Downer, C.W. Bielawski, G. Bersuker, J.C. Lee, and S.K. Banerjee, *J. Cryst. Growth* 334, 126–133 (2011).
12. J.H. Yum, T. Akyol, M. Lei, T. Hudnall, G. Bersuker, M. Downer, C.W. Bielawski, J.C. Lee, and S.K. Banerjee, *J. Appl. Phys.* 109, 064101–064104 (2011).
13. P. Sivasubramani, T.J. Park, B.E. Coss, A. Lucero, J. Huang, B. Brennan, Y. Cao, D. Jena, H. Xing, R.M. Wallace, and J. Kim, *Phys. Stat. Sol. Rapid Res. Lett* 6, 22–24 (2012).
14. A. Malmros, H. Blanck, and N. Rorsman, *Semicond. Sci. Technol.* 26, 075006 (2011).
15. C.L. Hinkle, M. Milojevic, E.M. Vogel, and R.M. Wallace, *Appl. Phys. Lett.* 95, 3–151905 (2009).
16. C.-T. Lee, H.-W. Chen, and H.-Y. Lee, *Appl. Phys. Lett.* 82, 4304–4306 (2003).
17. A. Fontserre, A. Perez-Tomas, V. Banu, P. Godignon, J. Millan, H. De Vleeschouwer, J. M. Parsey, P. Moens, *24th Int. Symp. Power Semicond. Devices and ICs (ISPSD)* pp. 37–40, (2012).
18. M. Lachab, M. Sultana, H. Fatima, V. Adivarahan, Q. Fareed, and M.A. Khan, *Semicond. Sci. Technol.* 27, 125001 (2012).